DALTON
FULL PAPER

Carbonyl sulfide insertion into Group 2 metal–isopropoxide bonds; synthesis and crystal structures of $[\mathrm{Mg(OCSOPr^i)_2(Pr^iOH)_4}]\cdot 2\mathrm{Pr^iOH}$ and $[\{\mathrm{Sr(OCSOPr^i)_2(Pr^iOH)_2}\}_n]$

Izoldi K. Bezougli,[a] Alan Bashall,[b] Mary McPartlin[b] and D. Michael P. Mingos[a]

[a] *Department of Chemistry, Imperial College of Science Technology and Medicine, South Kensington, London, UK SW7 2AY*

[b] *School of Applied Chemistry, University of North London, Holloway Road, London, UK N7 8DB*

The insertion reactions of COS into the metal–alkoxide bonds of some alkaline-earth metals have been investigated. The resulting compounds have been studied spectroscopically (IR, ^{1}H and ^{13}C NMR), and by analytical techniques (TGA). The crystal structures of the strontium complex $[\{\mathrm{Sr(OCSOPr^i)_2(Pr^iOH)_2}\}_n]$ and the magnesium complex $[\mathrm{Mg(OCSOPr^i)_2(Pr^iOH)_4}]\cdot 2\mathrm{Pr^iOH}$ have shown that whereas the former has a three dimensional structure the latter is monomeric.

The renewed interest in the chemistry of alkaline-earth-metal complexes can be attributed primarily to their potential use as molecular precursors in the preparation of thin films *via* metal organic chemical vapour deposition (MOCVD), for electroceramics such as superconductors and other speciality electronic materials.[1] Also, in the course of the understanding of their co-ordination chemistries several researchers have recently reported some significant developments in the chemistry of these materials, for example the structural characterisation of a wide range of organomagnesium complexes,[2] the facile cleavage of a wide range of organic ligands by the Group 2 metals and their complexation and characterisation of Group 2 metal alkoxides and β-diketonates.[3] Although several papers have examined the effects of different solvents on the volatility and reactivity of alkaline-earth-metal alkoxides,[4] the insertion reactions of small unsaturated molecules such as SO_2, CO_2, COS and CS_2 with alkaline-earth-metal alkoxides have been relatively neglected compared with the corresponding reactions with transition metals.[5–8] This may be attributed to the difficulty of synthesizing and handling Group 2 metal alkoxides which often led to their poor characterisation.[9] The first example of such an insertion compound to be structurally characterised was $[\{\mathrm{Ca(O_2SOMe)_2(MeOH)_2}\}_n]$,[10] resulting from the insertion of SO_2 into the calcium–methoxide bonds and later we also described the thiocarbonato-bridged dimer $[\{\mathrm{Ca(OCSOMe)_2(MeOH)_3}\}_2]$ resulting from the insertion reaction of COS into the calcium–methoxide bonds.[11] More recently we reported the crystal structure of the magnesium and strontium ethoxide analogues $[\mathrm{Mg(OCSOEt)_2(EtOH)_4}]$ **1** and $[\mathrm{Sr_3(OCSOEt)_6(EtOH)_8}]$ **2**,[12] and in this paper we report the extension of this research to the two Group 2 metal thiocarbonato isopropoxides $[\mathrm{Mg(OCSOPr^i)_2(Pr^iOH)_4}]$ **3** and $[\{\mathrm{Sr(OCSOPr^i)_2(Pr^iOH)_2}\}_n]$ **4**. The structures of **3** and **4** have been confirmed by single crystal X-ray crystallography.

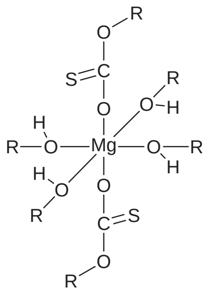

1, R = Et
3, R = $\mathrm{Pr^i}$

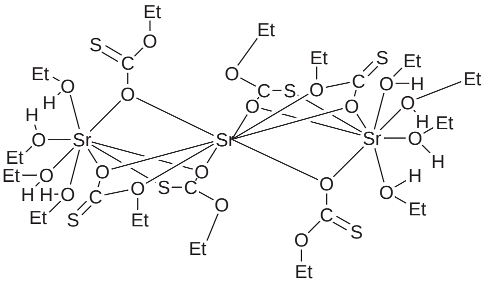

2

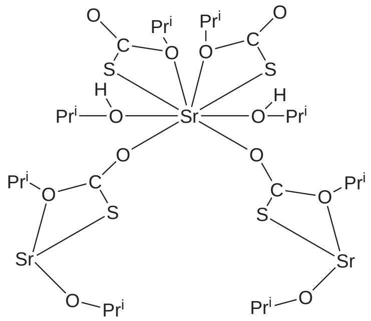

4

Results and Discussion

The two thiocarbonato complexes **3** and **4** were synthesized in a similar way to that described previously for **1** and **2**.[1] The crystalline $\mathrm{Pr^iOH}$-solvated metal isopropoxides $[\{\mathrm{Mg(OPr^i)_2(Pr^iOH)_4}\}_n]$ and $[\{\mathrm{Sr(OPr^i)_2(Pr^iOH)_4}\}_n]$ were suspended in $\mathrm{Pr^iOH}$ and COS bubbled through the suspension at room temperature to give an exothermic reaction which reached completion within 10 min. The products were isolated as colourless crystals after reducing the volume of the solvent. On the basis of single-crystal X-ray studies, analytical data and spectroscopic measurements, the products have been formulated as the monomeric and polymeric thiocarbonato complexes $[\mathrm{Mg(OCSOPr^i)_2(Pr^iOH)_4}]$ **3** and $[\{\mathrm{Sr(OCSOPr^i)_2(Pr^iOH)_2}\}_n]$ **4**, respectively. Complexes **3** and **4** are moisture sensitive, but may be

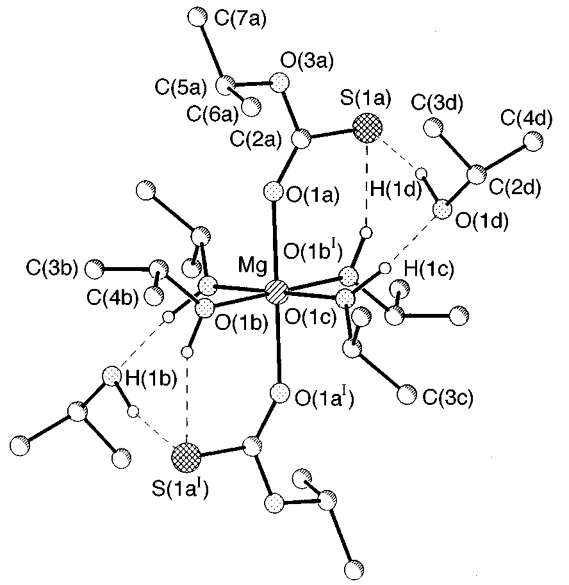

Fig. 1 Molecular structure of $[\mathrm{Mg(OCSOPr^i)_2(Pr^iOH)_4}]\cdot 2\mathrm{Pr^iOH}$ **3**, formed by the insertion of COS into the M–O bonds of magnesium isopropoxide

Table 1 Selected bond lengths (Å) and angles (°) for complex **3**

Mg–O(1b$^{\mathrm{I}}$)	2.060(2)	Mg–O(1b)	2.060(2)
Mg–O(3a)	2.060(2)	Mg–O(3a$^{\mathrm{I}}$)	2.060(2)
Mg–O(1c)	2.067(3)	Mg–O(1c$^{\mathrm{I}}$)	2.067(3)
S(1a)–C(2a)	1.712(4)	C(2a)–O(3a)	1.238(4)
C(2a)–O(4a)	1.333(4)	O(4a)–C(5a)	1.459(4)
C(5a)–C(6a)	1.492(6)	C(5a)–C(7a)	1.501(5)
O(1b)–C(2b)	1.442(4)	C(2b)–C(3b)	1.494(6)
C(2b)–C(4b)	1.507(6)	O(1c)–C(2c)	1.438(5)
C(2c)–C(4c)	1.500(6)	C(2c)–C(3c)	1.505(6)
O(1d)–C(2d)	1.429(6)	C(2d)–C(4d)	1.455(8)
C(2d)–C(3d)	1.472(7)		
O(1b$^{\mathrm{I}}$)–Mg–O(1b)	180.0	O(1b$^{\mathrm{I}}$)–Mg–O(3a)	87.32(9)
O(1b)–Mg–O(3a)	92.68(9)	O(1b$^{\mathrm{I}}$)–Mg–O(3a$^{\mathrm{I}}$)	92.68(9)
O(1b)–Mg–O(3a$^{\mathrm{I}}$)	87.32(9)	O(3a)–Mg–O(3a$^{\mathrm{I}}$)	180.0
O(1b$^{\mathrm{I}}$)–Mg–O(1c)	90.24(11)	O(1b)–Mg–O(1c)	89.76(11)
O(3a)–Mg–O(1c)	89.46(10)	O(3a$^{\mathrm{I}}$)–Mg–O(1c)	90.54(10)
O(1b$^{\mathrm{I}}$)–Mg–O(1c$^{\mathrm{I}}$)	89.76(11)	O(1b)–Mg–O(1c$^{\mathrm{I}}$)	90.24(11)
O(3a)–Mg–O(1c$^{\mathrm{I}}$)	90.54(10)	O(3a$^{\mathrm{I}}$)–Mg–O(1c$^{\mathrm{I}}$)	89.46(10)
O(1c)–Mg–O(1c$^{\mathrm{I}}$)	180.0	C(2a)–O(3a)–Mg	144.5(2)
C(2b)–O(1b)–Mg	137.8(2)	C(2c)–O(1c)–Mg	128.9(2)

Symmetry transformation used to generate equivalent atoms: I $-x$, $-y$, $-z$.

stored indefinitely under an inert atmosphere at room temperature without losing COS, although some reversible desolvation occurs. They are soluble in alcohols, co-ordinating and polar organic solvents, but have poor solubilities in hydrocarbons.

Crystal structures

$[\mathrm{Mg(OCSOPr^i)_2(Pr^iOH)_4}]\cdot 2\mathrm{Pr^iOH}$ 3. The X-ray structural analysis established a discrete monomeric molecule as the insertion product of reaction of COS with $[\mathrm{Mg(OPr^i)_2(Pr^iOH)_4}]$. The centrosymmetric structure is shown in Fig. 1 and selected bond lengths and angles are listed in Table 1. Insertion of the COS into two Mg–OPr^i bonds has resulted in two *trans*-monodentate isopropyl thiocarbonato ligands bonded through the oxygen atom of the COS group, and an octahedral co-ordination is completed by four oxygen atoms of equatorial Pr^{i}OH molecules. The overall structure is very similar to that of complex 1 formed by insertion of COS into Mg–OEt, but unlike 1 the solid state structure of **3** incorporates two additional alcohol molecules per asymmetric unit. Each of these symmetry related Pr^{i}OH molecules forms hydrogen bonds with the sulfur atom of an axial $\mathrm{OCS(OPr^i)^-}$ ligand [O(H1d)···S(1a) 2.188, O(H1b$^{\mathrm{I}}$)···S(1a) 2.150 Å] and the hydrogen of an equatorial Pr^{i}OH ligand [H(1c)···O(1d) 2.650 Å] thus forming a bridge between these two ligands (Fig. 1).

In the structure of complex **1** the symmetry related Mg–OCSOEt bond lengths (Mg–O 2.036 Å) were found to be significantly shorter than the two independent Mg–O(H)Et lengths [mean 2.083(2) Å]. In the present study all the Mg–O bond lengths in **3** are very similar lying in the range 2.060(2)–2.067(3) Å; the apparent lengthening of the Mg–O bond to the alkyl thiocarbonato ligand in **3** may be attributed to steric factors associated with the greater bulk of the isopropyl group compared to the ethyl group in **1**.

$[\{\mathrm{Sr(OCSOPr^i)_2(Pr^iOH)_2}\}_n]$ 4. X-Ray structural analysis of complex **4**, $[\{\mathrm{Sr(OCSOPr^i)_2(Pr^iOH)_2}\}_n]$, established the presence of a polymeric material. Each strontium atom lies on a site of C_2 symmetry and is co-ordinated by oxygen atoms of two symmetry related Pr^{i}OH ligands [O(1b) and O(1b$^{\mathrm{III}}$)] and is chelated by the sulfur and oxygen atoms of two symmetry related isopropyl thiocarbonato ligands as illustrated in Fig. 2. Selected bond lengths and angles are listed in Table 2. Eight-co-ordination of the strontium centre is completed by bonds from two oxygen atoms [O(3a$^{\mathrm{I}}$) and O(13a$^{\mathrm{II}}$)] of two $\mathrm{OCS(OPr^i)^-}$ ligands on adjacent strontium atoms, generated by the crystal symmetry, resulting in a three-dimensional polymeric structure. This contrasts with the discrete trimeric molecules $[\mathrm{Sr_3(OCSOEt)_6(EtOH)_8}]$ **2** formed from the insertion reaction of COS with strontium ethoxide. Polymer formation in **4** may be facilitated by the co-ordination of only two relatively bulky Pr^{i}OH molecules to each strontium centre compared to the four smaller ethanol molecules which co-ordinate each of the terminal strontium atoms in **2**.

Bidentate bonding of an alkyl thiocarbonato ligand *via* sulfur and oxygen atoms has been observed previously for the COS insertion products $[\{\mathrm{Ca(OCSOMe)_2(MeOH)_3}\}_2]$[11] and $[\mathrm{Sr_3(OCSOEt)_6(EtOH)_8}]$ **2**, and in each of these it is the oxygen of the COS group which is involved. In contrast, the alkyl thiocarbonato ligand in **4** forms a chelate ring involving the sulfur and isopropyl oxygen atoms of $\mathrm{OCS(OPr^i)^-}$. The Sr–O distance in the sulfur–oxygen chelate ring of **4** is considerably longer [Sr–O(4a) 2.796(3) Å] than that in **2** [Sr–O 2.785(5) Å], consistent with the weaker donor character of the 'ether' oxygen in $\mathrm{OCS(OPr^i)^-}$ in **4**; the Sr–S(1a) length of 3.061(1) Å in the chelate ring of **4** is slightly longer than that of 3.025(3) Å in **2**.

Infrared spectroscopy

The main stretching vibrations of complexes **1**–**4** are summarised in Table 3 and have been assigned on the basis of previously published infrared data for similar compounds.[13] In view of their similar crystal structures it is not surprising that **1** and **3** exhibit similar stretching vibrations in their infrared spectra. Both complexes are co-ordinated in a monodentate fashion to the terminal oxygen of the $\mathrm{(OCS)OR^-}$ ligand, exhibiting only one set of vibrations for the ligand. The band at 1551 cm^{-1} of **3** has been assigned to the ν(C=O) stretching mode of the COS moiety and the band at 1162 cm^{-1} to the ν(C=S) stretching mode. These bands are similar to those observed for **1** at 1554 and 1174 cm^{-1}, respectively. The IR spectra of complexes **2** and **4** are clearly different and imply dissimilar alkyl thiocarbonato co-ordination modes. Complex **4** shows only one ν(CO) at 1579 cm^{-1} and a ν(C–S) stretch at 950 cm^{-1}. In contrast, **2** exhibits a more complicated infrared spectrum, with three CO stretching frequencies at 1620, 1598 and 1568 cm^{-1}, suggesting multiple co-ordination modes for the $\mathrm{OCS(OEt)^-}$ ligand. Nevertheless, the infrared spectra were measured as solids and therefore the

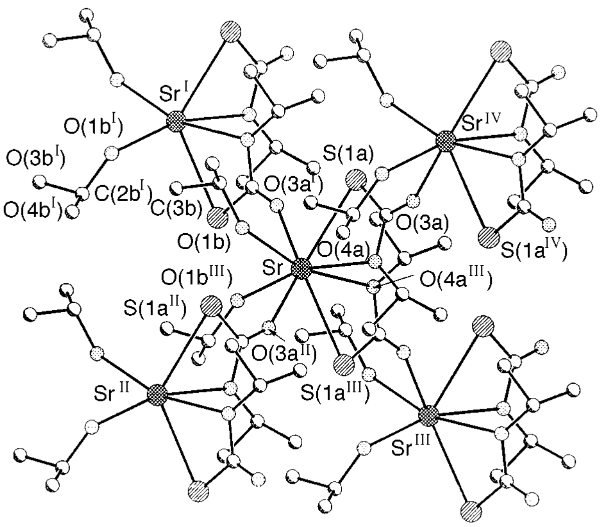

Fig. 2 Part of the three dimensional structure of the COS insertion product [{Sr(OCSOPr^i)$_2$(Pr^{i}OH)$_2$}$_n$] **4**, showing the unique μ$_3$-bridging mode adopted by the alkylthiocarbonato ligand

Table 2 Selected bond lengths (Å) and angles (°) for complex **4**

Sr–O(3a$^{\text{I}}$)	2.505(3)	Sr–O(3a$^{\text{II}}$)	2.505(3)
Sr–O(1b$^{\text{III}}$)	2.540(3)	Sr–O(1b)	2.540(3)
Sr–O(4a)	2.796(3)	Sr–O(4a$^{\text{III}}$)	2.796(3)
Sr–S(1a)	3.0607(13)	Sr–S(1a$^{\text{III}}$)	3.0607(13)
S(1a)–C(2a)	1.703(4)	C(2a)–O(3a)	1.213(5)
C(2a)–O(4a)	1.370(5)	O(3a)–Sr$^{\text{IV}}$	2.505(3)
O(4a)–C(5a)	1.478(5)	C(5a)–C(6a)	1.481(7)
C(5a)–C(7a)	1.492(7)	O(1b)–C(2b)	1.422(5)
C(2b)–C(3b)	1.473(8)	C(2b)–C(4b)	1.482(8)
O(3a$^{\text{I}}$)–Sr–O(3a$^{\text{II}}$)	140.3(2)	O(3a$^{\text{I}}$)–Sr–O(1b$^{\text{III}}$)	70.92(11)
O(3a$^{\text{II}}$)–Sr–O(1b$^{\text{III}}$)	81.14(11)	O(3a$^{\text{I}}$)–Sr–O(1b)	81.14(11)
O(3a$^{\text{II}}$)–Sr–O(1b)	70.92(11)	O(1b$^{\text{III}}$)–Sr–O(1b)	89.9(2)
O(3a$^{\text{I}}$)–Sr–O(4a)	125.10(9)	O(3a$^{\text{II}}$)–Sr–O(4a)	86.56(10)
O(1b$^{\text{III}}$)–Sr–O(4a)	163.43(9)	O(1b)–Sr–O(4a)	96.57(11)
O(3a$^{\text{I}}$)–Sr–O(4a$^{\text{III}}$)	86.56(10)	O(3a$^{\text{II}}$)–Sr–O(4a$^{\text{III}}$)	125.10(9)
O(1b$^{\text{III}}$)–Sr–O(4a$^{\text{III}}$)	96.57(11)	O(1b)–Sr–O(4a$^{\text{III}}$)	163.43(9)
O(4a)–Sr–O(4a$^{\text{III}}$)	81.45(14)	O(3a$^{\text{I}}$)–Sr–S(1a)	74.18(7)
O(3a$^{\text{II}}$)–Sr–S(1a)	125.66(8)	O(1b$^{\text{III}}$)–Sr–S(1a)	144.78(8)
O(1b)–Sr–S(1a)	80.21(9)	O(4a)–Sr–S(1a)	51.72(6)
O(4a$^{\text{III}}$)–Sr–S(1a)	85.81(7)	O(3a$^{\text{I}}$)–Sr–S(1a$^{\text{III}}$)	125.66(8)
O(3a$^{\text{II}}$)–Sr–S(1a$^{\text{III}}$)	74.18(7)	O(1b$^{\text{III}}$)–Sr–S(1a$^{\text{III}}$)	80.21(9)
O(1b)–Sr–S(1a$^{\text{III}}$)	144.78(8)	O(4a)–Sr–S(1a$^{\text{III}}$)	85.81(7)
O(4a$^{\text{III}}$)–Sr–S(1a$^{\text{III}}$)	51.72(6)	S(1a)–Sr–S(1a$^{\text{III}}$)	125.62(5)
C(2a)–S(1a)–Sr	88.1(2)	C(2a)–O(3a)–Sr$^{\text{IV}}$	154.5(3)
C(2a)–O(4a)–Sr	106.9(2)	C(5a)–O(4a)–Sr	135.9(2)
C(2b)–O(1b)–Sr	135.0(3)		

Symmetry transformations used to generate equivalent atoms: I $x+\frac{1}{4}$, $-y+\frac{1}{4}$, $z+\frac{1}{4}$; II $-x-\frac{1}{4}$, $y-\frac{1}{4}$, $z+\frac{1}{4}$; III $-x$, $-y$, z; IV $x-\frac{1}{4}$, $-y+\frac{1}{4}$, $z-\frac{1}{4}$.

Table 3 Characteristic infrared data (cm^{-1}) for complexes **1–4**. The spectra were obtained in the solid state as Nujol mulls

Complex	ν(CO)	ν(C=S)	ν(C–S)	ν(C–OR)
1	1554	1174	—	1091, 1050
2	1620, 1598, 1568	1176, 1152	972, 946	1051
3	1551	1162	—	1095
4	1579	—	950	1103, 1066, 1041

above analysis has to be treated with some caution because of possible solid state effects.

Nuclear magnetic resonance

The ^{1}H and ^{13}C-{^{1}H} NMR spectroscopic studies for complexes **1–4** were made in (CD$_3$)$_2$SO solution and are summarised in Tables 4 and 5, respectively.

Table 4 Proton NMR data (δ) for complexes **1–4** in (CD$_3$)$_2$SO

Complex	OH of ROH	CH$_2$ or CH of OCSOR	CH$_2$ or CH of ROH	CH$_3$ of OCSOR/ ROH
1	4.41 (t)	3.74 (q)	3.41 (dq)	1.04 (t)
2	4.39 (t)	3.80 (q)	3.42 (dq)	1.04 (t)
3	4.40 (d)	4.65 (q)	3.77 (dq)	1.05 (d)
4	4.44 (d)	4.75 (m)	3.78 (dq)	1.09/1.05 (d)

Table 5 ^{13}C-{^{1}H} NMR data (δ) for complexes **1–4** in (CD$_3$)$_2$SO

Complex	OCSOR	CH$_2$ or CH of OCSOR	CH$_2$ or CH of ROH	CH$_3$ of ROH	CH$_3$ of OCSOR
1	183.42	59.53	56.66	19.19	15.62
2	184.76	60.13	56.67	19.19	15.15
3	183.53	65.99	63.12	26.59	23.60
4	185.59	67.73	63.33	26.58	23.46

The proton NMR studies clearly differentiate the alcohol and alkyl thiocarbonato ligands. A doublet of quartets for the CH of the co-ordinated Pr^{i}OH molecules was observed at δ 3.77 for **3** and 3.78 for **4**, while a multiplet at δ 4.65 for **3** and 4.75 for **4** was assigned to the CH of the isopropyl thiocarbonato moieties. The two different CH$_3$ environments of the Pr^{i}OH and isopropyl thiocarbonato moieties appeared in the same region as two superimposed doublets for **3** (δ 1.05) and as two distinct doublets for **4** (δ 1.05 and 1.09). Similar proton NMR assignments were obtained for **1** and **2**.[12]

The ^{13}C-{^{1}H} NMR spectra of complexes **1–4** were assigned in a similar manner. A characteristic signal for the thiocarbonato carbon, OCS(OR)$^-$, was observed at higher chemical shifts at around δ 184 for all complexes. The data clearly reveal the presence of two distinct types of alkyl environments, one corresponding to the bound alcohol molecules and one corresponding to the alkyl thiocarbonato ligands. Darensbourg *et al.*[14,15] described similar chemical shift positions for COS insertion products with tungsten alkoxides.

Thermogravimetric analysis (TGA) and differential scanning calorimetry (DSC)

The differential scanning calorimetry (DSC) trace for the magnesium complex **3** shows an endothermic peak between 19 and 130 °C. This is mirrored in the TGA plot with a 75% weight loss, corresponding to loss of the co-ordinated Pr^{i}OH and the loss of the COS molecules. The subsequent weight loss percentage *ca.* 15% represents the decomposition of Mg(OPr^i)$_2$ to MgO between 130 and 800 °C leaving a residue of 9.30% (calc. 9.05%). A similar DSC trace to that of **3** was obtained for compound **4**. An endotherm between 100 and 160 °C corresponds to a 40% weight loss on the TGA plot and is assigned to the loss of the COS molecules. The subsequent weight loss of *ca.* 30% represents the decomposition of Sr(OPr^i)$_2$ to SrO between 160 and 800 °C leaving a residue of 30.1% (calc. 31.82%). The TGA plot of **4** between 20 and 100 °C suggests that all the Pr^{i}OH molecules attached to the metal were lost before the measurement was made. Similarly, from the residue of the TGA of **3** it is deduced that only three molecules of Pr^{i}OH remained in the solid sample when the TGA analysis was made. This may be due to the fact that the compounds were exposed to air for some seconds before they were transferred to the TGA apparatus for the measurements. The observation of an endotherm for **3** and an exotherm for **4** in closely related complexes suggests that the thermodynamics of the decomposition process is sensitive to the nuclearity of the complex and the mode of co-ordination of the isopropyl thiocarbonato ligand. Similar simultaneous thermal analysis (STA) was obtained for **1** and **2**.[12] In all cases the alcohol molecules were released first below 100 °C, followed by the COS molecules at *ca.* 140 °C, leaving a residue of the metal oxide above 700 °C.

Mass spectrometric studies using fast atom bombardment (FAB) (positive and negative ion) techniques for all complexes **1–4** yielded complicated fragmentation patterns. Molecular ions were not observed probably because of the poor volatilities and thermal stabilities of these complexes. Nevertheless, the complexes exhibited fragments which have been assigned in the Experimental section.

Conclusion

The research described in this paper has demonstrated that the insertion of COS into Group 2 metal alkoxide bonds leads to a range of crystalline derivatives which are reasonably air stable and soluble in organic solvents. Both IR and NMR techniques were very useful in characterising these complexes. The IR spectra revealed different co-ordination modes of the $COS(OR)^-$ ligand, while in the ^1H and ^{13}C-$\{^1H\}$ NMR spectra the different OR^- and $COS(OR)^-$ ligands were clearly differentiated. The NMR spectra confirmed the stoichiometries of the compounds. The thermogravimetric results indicate that the insertion of the COS molecule may be reversed at high temperatures.

The crystallographic structural determinations of complexes **3** and **4** together with those previously studied, **1** and **2**, have revealed a variety of bonding motifs. The $OCS(OR)^-$ ligand appears to be a flexible ligand which can use its alternative donor sites and bridging modes to co-ordinate to a wide range of metals and thereby form a series of crystalline derivatives with low molecular weights. Moving down the group from Mg^{2+} in **3** to Sr^{2+} in **4**, the increase in the ionic radii of the metal ion [from Mg^{2+} (0.72) to Sr^{2+} (1.18 Å)][16] leads to a preference for higher co-ordination numbers which are achieved by oligomerisation or polymerisation processes. That results in the introduction of the S and OR groups into the co-ordination sphere in order to make up the co-ordination number. This was also observed in the previously described complexes **1** and **2**. Therefore, the $(OCS)OR^-$ ligand adopts a monodentate co-ordination mode in **1** and **3** and bidentate bridging co-ordination modes in **2** and **4**. The different co-ordination modes adopted by the $OCS(OEt)^-$ ligand in **1** and **2** have been previously discussed.[12] In the polymeric structure associated with **4** a new bonding mode is observed which involves a novel ligand bridge **A** and, for the first time, all three potential donor atoms of the ligand are simultaneously bonded to metal ions.

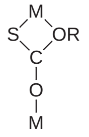

(A)

Experimental

General procedures

All manipulations were carried out under an atmosphere of dry nitrogen using standard glove-box (Miller-Howe FF160) and Schlenk techniques. All solvents were rigorously dried and deoxygenated by standard procedures. The samples for NMR, infrared studies and thermogravimetric analyses were handled in a glove-box, but those for microanalyses were not. The complexes desolvate when exposed to air and that has led to some differences concerning the extent to which Pr^iOH molecules of crystallisation were detected by the spectroscopic and analytical techniques.

Instrumentation

Infrared spectra were recorded on a Perkin-Elmer FTIR 1720 spectrometer using Nujol mulls between 25 × 4 mm CsI plates. The Nujol was dried with 4 Å molecular sieves prior to use (and stored in a glove-box); the samples were protected from the atmosphere by an O-ring-sealed Presslok holder (Aldrich Chemicals). The NMR spectra were recorded on a JEOL GS 270 MHz spectrometer; ^1H NMR was referenced internally to the residual ^1H impurity present in the deuteriated solvent. Chemical shifts are recorded in parts per million (δ) relative to $SiMe_4$ (δ 0) using $(CD_3)_2SO$ (δ 2.52), ^{13}C NMR spectra to $(CD_3)_2SO$ (δ 40.6). Controlled thermal analyses of the complexes were investigated using a Polymer Laboratories 1500H simultaneous thermal analyser, controlled by an OmniPro 486DX-33 personal computer. The mass of the samples was between 10 and 20 mg. The measurements were carried out in alumina crucibles under an atmosphere of flowing (25 $cm^3\ min^{-1}$) nitrogen gas, using heating rates of 5 °C min^{-1}.

Starting materials

Strontium granules and dibutylmagnesium from Aldrich Chemicals Co. were used as received.

Preparations

Tetra(isopropylalcohol)bis(*O*-isopropyl thiocarbonato)magnesium, $[Mg(OCSOPr^i)_2(Pr^iOH)_4]$ 3. Dibutylmagnesium in heptane (10 cm^3, 1 M, 10 mmol) was added to Pr^iOH (30 cm^3) at −40 °C resulting in an exothermic reaction. The reaction mixture was slowly warmed to room temperature, the volume of the solvent was reduced until all the heptane was removed and precipitation of a white solid $[\{Mg(OPr^i)_2(Pr^iOH)_4\}_n]$ was observed. Addition of Pr^iOH (30 cm^3) resulted in a suspension of the magnesium isopropoxide. Carbonyl sulfide gas was bubbled through the suspension at room temperature for 30 min. The solution was stirred for 12 h until all the alkoxide had dissolved to afford a yellow solution. A crystalline solid was isolated after cooling the solution to −20 °C (yield: 3.80 g, 75.7%) (Found: C, 46.4; H, 9.1. Calc. for $C_{20}H_{48}MgO_9S_2$: C, 46.9; H, 9.3%) [analysis based on $Mg(OCSOPr^i)_2(Pr^iOH)_4\cdot H_2O$]. IR ($cm^{-1}$) (Nujol): 3369s (br), 3197s (br), 1551s, 1342w, 1301w, 1261w, 1162s, 1095s, 950m, 875w, 817m, 694m, 524w and 437w. NMR [$(CD_3)_2SO$, 20 °C]: ^1H (270 MHz), δ 4.65 [q, $OCSOCH(CH_3)_2$, 2 H], 4.40 [d, $(CH_3)CHOH$, 4 H], 3.77 [dq, $(CH_3)_2CHOH$, 4 H] and 1.05 (d, CH_3, $OCSOPr^i/Pr^iOH$, 36 H); ^{13}C-$\{^1H\}$ (67.94 MHz), δ 183.53 ($OCSOPr^i$), 65.99 [$OCSOCH(CH_3)_2$], 63.12 [$(CH_3)_2CHOH$], 26.59 [$CH(CH_3)_2OH$] and 23.60 [$OCSOCH(CH_3)_2$]. Mass spectrum: (positive-ion FAB), *m/z* 120, $(OCS)_2$; 152, $(OCSO)_2$; 290, $[Mg(OCSOPr^i)_2(OC)]$ and 443, $[Mg(OCSOPr^i)_2(Pr^iOH)_3]^+$; (negative-ion FAB), *m/z* 175, $[Mg(OCSO)_2]^-$; 192, $[Mg(OCSO)_2O]$ and 223, $[Mg(OCSO)_2O_3]^-$.

Di(isopropyl alcohol)bis(*O*-isopropyl thiocarbonato)strontium, $[\{Sr(COSOPr^i)_2(Pr^iOH)_2\}_n]$ 4. Strontium metal (0.97 g, 11.07 mmol) was suspended in Pr^iOH (40 cm^3) and the mixture was stirred for 12 h at room temperature resulting in dissolution of the metal and evolution of hydrogen gas, yielding a transparent slightly purple solution. The solution was filtered and COS gas bubbled through the clear solution for 15 min at room temperature, resulting in an exothermic reaction to give a clear yellow solution. The solution was stirred for 1 h and a crystalline solid isolated by cooling the solution to −20 °C (yield: 3.81 g, 77.3%) (Found: C, 36.6; H, 5.9. Calc. for $C_{14}H_{30}O_6S_2Sr$: C, 37.7; H, 6.8%) [analysis is based on $Sr(OCSOPr^i)_2(Pr^iOH)_2$]. IR (cm^{-1}) (Nujol): 3295m, 1579m, 1303w, 1159m, 1147m, 1103m, 1066m, 1041m, 973w, 950s, 917m, 852m, 815m, 723m and 682w. NMR [$(CD_3)_2SO$, 20 °C]: ^1H (270 MHz), δ 4.75 [m, $OCSOCH(CH_3)_2$, 2 H], 4.44 [d, $(CH_3)_2CHOH$, 2 H], 3.78 [dq, $(CH_3)_2CHOH$, 2 H], 1.09 [d, $OCSOCH(CH_3)_2$, 6 H] and 1.05 [d, $(CH_3)_2CHOH$, 6 H]; ^{13}C-$\{^1H\}$ (67.94 MHz), δ 185.59 ($OCSOR$), 67.73 [$OCSOCH(CH_3)_2$], 63.33 [$(CH_3)_2CHOH$], 26.58 [$(CH_3)_2CHOH$] and 23.46 [$OCSOCH(CH_3)_2$]. Mass spectrum: (positive-ion FAB), *m/z* 88, $[Sr]^+$; 105, $[SrO]^+$; 120, $[SrO_2]$; 165, $[Sr(OCSO)]^+$ and 267, $[Sr(OCSOPr^i)(Pr^iOH)]^+$.

Table 6 Crystal data and structure refinement for complexes **3** and **4**

	3	**4**
Formula	$C_{26}H_{62}MgO_{10}S_2$	$C_{14}H_{30}O_6S_2Sr$
M_r	623.19	446.12
Crystal system	Monoclinic	Orthorhombic
Space group	$P2_1/n$	$Fdd2$
a/Å	11.332(2)	17.283(3)
b/Å	14.535(2)	15.544(5)
c/Å	11.538(2)	15.769(6)
β/°	93.800(9)	
U/Å^3	1896.2(5)	4236(2)
Z	2	8
D_c/Mg m^{-3}	1.091	1.399
F(000)	684	1856
Crystal size/mm	0.24 × 0.40 × 0.50	0.56 × 0.38 × 0.36
λ/Å	0.710 73	0.710 73
μ(Mo-Kα)/mm^{-1}	0.200	2.764
θ Range/°	2.26 to 25.00	2.18 to 25.09
hkl Ranges	−13 to 13, −17 to 17, −13 to 13	−20 to 20, −18 to 18, −18 to 18
Reflections collected	7028	1964
Unique reflections	3342	1890
Data, restraints, parameters	3339, 0, 186	1889, 1, 110
Goodness of fit on F^2, S	1.017	1.039
Transmission factors (minimum/maximum)	0.187/0.982	0.254/0.356
Final $R1$, $wR2$		
$I > 2\sigma(I)$	0.0631, 0.1538	0.0338, 0.0735
all data	0.1094, 0.1836	0.0411, 0.0765
Weighting, w^{-1}	$\sigma^2(F_o)^2 + (0.082\,60P)^2 + 1.0358P$	$\sigma^2(F_o)^2 + (0.049\,95P)^2 + 0.00P$
Largest peak and hole/e Å^{-3}	0.609, −0.353	0.739, −0.347

$S = [\Sigma w(F_o^2 - F_c^2)^2/(n - p)]^{\frac{1}{2}}$, $R1 = \Sigma||F_o| - |F_c||/\Sigma|F_o|$, $wR2 = \Sigma w(F_o^2 - F_c^2)^2/\Sigma[w(F_o^2)^2]^{\frac{1}{2}}$, $P = [\max(F_o^2, 0) + 2(F_c^2)]/3$ where n = number of reflections and p = total number of parameters.

X-Ray crystallography

Data were collected using a Siemens P4 diffractometer equipped with a Siemens LT2 low temperature device with graphite monochromated radiation Mo-Kα using ω–2θ scans at 198 K. No significant decay in the intensity of three standard reflections measured after every 100 was observed. The data were corrected for Lorentz-polarisation factors and for absorption (ψ scans). The crystal data, data collection and refinement details are summarised in Table 6.

Both structures were solved by direct methods and in each case all non-hydrogen atoms were located from subsequent Fourier-difference syntheses. All non-hydrogen atoms were assigned anisotropic thermal parameters and refined using full-matrix least squares on F_o^2.[17] The hydrogen atoms for each of the compounds were included at calculated positions with C–H bond distances of 1.00 and 0.98 Å for the methine and methyl groups, respectively. The hydroxyl hydrogens of both compounds were located from Fourier-difference syntheses. During refinement all the hydrogens were allowed to ride on their parent atom (the positional parameters of the directly located hydrogens were not refined) and were assigned isotropic thermal parameters equal to 1.2 U_{eq} of the parent atom for the methine groups and 1.5 U_{eq} for the methyl and hydroxyl groups.

CCDC reference number 186/1051.

See http://www.rsc.org/suppdata/dt/1998/2665/ for crystallographic files in .cif format.

Acknowledgements

The EPSRC is thanked for financial support and BP plc for endowing D. M. P. M.'s Chair.

References

1 D. C. Bradley, *Polyhedron*, 1994, **13**, 1111.

2 P. R. Markies, O. S. Akkerman, F. Bickelhaupt, W. J. J. Smeets and A. L. Spek, *Adv. Organomet. Chem.*, 1991, **32**, 147.

3 S. R. Drake, M. H. Chisholm, K. G. Caulton and J. C. Huffman, *Inorg. Chem.*, 1991, **31**, 1500; S. R. Drake, M. H. Chisholm, K. G. Caulton and K. Folting, *J. Chem. Soc.*, *Chem. Commun.*, 1990, 1345, 1498.

4 P. H. Dickenson, T. H. Geballe, A. Sanjurjo, D. Hildenbrand, G. Craig, M. Zisk, J. Collman, S. A. Banning and R. A. Sievers, *J. Appl. Phys.*, 1989, **66**, 444; C. I. M. A. Spee and A. Mackor, *Science of Technology of Thin Film Superconductors*, eds. R. D. McConnell and S. A. Wolf, New York, 1989, p. 281; S. Matsuno, F. Uchikawa and K. Yoshizaki, *Jpn. J. Appl. Phys.*, 1990, **29**, L947; J. M. Buriak, L. K. Cheatham, J. J. Graham, R. G. Gordon and A. R. Barron, *Mater. Res. Soc. Symp. Proc.*, 1991, **204**, 545.

5 G. J. Kubas, *Acc. Chem. Res.*, 1994, **27**, 183; W. A. Schenk, *Angew. Chem., Int. Ed. Engl.*, 1987, **26**, 98; R. Ros, G. Carturan and M. Graziani, *Transition Met. Chem.*, 1975, **1**, 13; G. R. Hughes, P. C. Minshall and D. M. P. Mingos, *Transition Met. Chem.*, 1979, **4**, 147; S. L. Randall, C. A. Miller, T. S. Janik, M. R. Churchill and J. D. Atwood, *Organometallics*, 1994, **13**, 141.

6 K. K. Panday, *Coord. Chem. Rev.*, 1995, **140**, 37.

7 D. J. Darensbourg and R. A. Kudarovski, *Adv. Organomet. Chem.*, 1983, **22**, 129; T. Tsuda, S. Sanada, K. Ueda and T. Saegusa, *Inorg. Chem.*, 1976, **15**, 2329; T. Yamamoto, M. Kuboto and A. Yamamoto, *Bull. Chem. Soc. Jpn.*, 1980, **53**, 680; M. H. Chisholm, W. W. Reichert, F. A. Cotton and C. A. Murillo, *J. Am. Chem. Soc.*, 1977, **99**, 1652.

8 J. A. Ibers, *Chem. Soc. Rev.*, 1982, **11**, 57; K. K. Pandey and H. L. Nigam, *Rev. Inorg. Chem.*, 1984, **6**, 69.

9 W. E. Lindsell, *Comprehensive Organometallic Chemistry*, eds. G. Wilkinson, F. G. A. Stone and E. Abel, Pergamon, Oxford, 1982, vol. 1, ch. 3.

10 V. C. Arunasalam, I. Baxter, M. B. Hursthouse, K. M. A. Malik, D. M. P. Mingos and J. C. Plakatouras, *J. Chem. Soc.*, *Chem. Commun.*, 1994, 2695.

11 V. C. Arunasalam, D. M. P. Mingos, J. C. Plakatouras, I. Baxter, M. B. Hursthouse and K. M. A. Malik, *Polyhedron*, 1995, **14**, 1105.

12 I. K. Bezougli, A. Bashall, M. McPartlin and D. M. P. Mingos, *J. Chem. Soc.*, *Dalton Trans.*, 1997, 287.

13 A. J. Goodsel and G. Blyholder, *J. Am. Chem. Soc.*, 1972, **94**, 6725.

14 D. J. Darensbourg, B. L. Mueller, C. J. Bischoff, S. S. Chojnacki and J. H. Reibenspies, *Inorg. Chem.*, 1991, **30**, 2418.

15 D. J. Darensbourg, K. M. Sanchez, J. H. Reibenspies and A. L. Rheingold, *J. Am. Chem. Soc.*, 1989, **111**, 7094.

16 T. P. Hanusa, *Chem. Rev.*, 1993, **93**, 1023.

17 SHELXTL, PC version 5.03, Siemens Analytical Instruments Inc., Madison, WI, 1994.

Received 6*th April* 1998; *Paper* 8/02595I